JOURNAL OF Materials CHEMISTRY

The novel open-framework uranium silicates $Na_2(UO_2)(Si_4O_{10})\cdot 2.1H_2O$ (USH-1) and $RbNa(UO_2)(Si_2O_6)\cdot H_2O$ (USH-3)

Xiqu Wang,* Jin Huang, Lumei Liu and Allan J. Jacobson

Department of Chemistry and Materials Research Science and Engineering Center, University of Houston, Houston, Texas, 77204-5641, USA. E-mail: xiqu.wang@mail.uh.edu; Fax: 713 7432787; Tel: 713 7432785

Received 30th October 2001, Accepted 17th January 2002
First published as an Advance Article on the web 29th January 2002

The new open-framework uranium silicates $Na_2(UO_2)(Si_4O_{10})\cdot 2.1H_2O$ (USH-1) and $RbNa(UO_2)(Si_2O_6)\cdot H_2O$ (USH-3) have been synthesized by hydrothermal reactions at 230 °C. USH-1 has a framework structure formed from silicate single layers cross-linked by interlayer UO_6 tetragonal bipyramids. The silicate layers consist of interconnected tetrahedral 4-rings and 8-ring voids. The 8-ring voids are lined up to form 1-dimensional channel systems in the framework. In contrast to the silicate layers of USH-1, individual 4-rings of silicate tetrahedra are found in USH-3 which are cross-linked by UO_6 tetragonal bipyramids to form an open framework.

Introduction

Crystalline materials with microporous structures are of interest for applications such as catalysis, ion-exchange and separation processes. By far the most classical and best known microporous silicates are zeolites that have open frameworks formed from interconnected SiO_4 and AlO_4 tetrahedra.[1] In the early nineteen eighties successful replacement of SiO_4 by PO_4 greatly increased the diversity of porous framework topologies.[2] Substitution of aluminium by other metals resulted in the discovery of a large number of open-framework metal phosphates with structures based on both tetrahedral and non-tetrahedral units. Particularly successful systems include gallium, molybdenum, vanadium and iron phosphates.[3] Recently synthesis studies of microporous phosphates were successfully extended to actinide metal phosphates.[4] In contrast, relatively less progress has been made in synthesis of the corresponding silicates.[5] A few prominent examples of porous transition metal silicates such as the titanium silicates ETS-4 and ETS-10 were found, however, to have remarkable absorption properties that may lead to important commercial applications.[6]

We are currently investigating the synthesis of transition metal silicates. Recently we reported two open-framework vanadium silicates $K_2(VO)(Si_4O_{10})\cdot H_2O$ (VSH-1) and $Cs_2(VO)(Si_6O_{14})\cdot 2H_2O$ (VSH-2) which were synthesized under hydrothermal conditions.[7] These two compounds and the closely related cavansite and pentagonite, dimorphs of the mineral $Ca(VO)(Si_4O_{10})\cdot 4H_2O$,[8] have a common structural feature, *i.e.*, open frameworks formed from silicate layers cross-linked by VO_5 tetragonal pyramids. Specifically, each VO_5 pyramid shares its basal oxygen corners with four SiO_4 tetrahedra. We are exploring the extension of this building principle by studying the substitution of $(VO_5)^{6-}$ pyramids by other coordination polyhedra that can share four corners in square planar geometry with the silicate tetrahedra. Examples of candidate bridging units include $(CuO_4)^{6-}$, $(TiO_5)^{6-}$, $(UO_6)^{6-}$, $(NbO_5F)^{6-}$ and $(ZrO_4F_2)^{6-}$. A new porous compound based on germanate tetrahedral chains cross-linked by NbO_5F octahedra has been synthesized recently in our lab.[9] A closely related zirconium germanate with ZrO_4F_2 octahedra linking germanate tetrahedral chains is also known.[10] The framework structure of ETS-4 may be considered as formed from double chains of silicate tetrahedra interconnected by TiO_5 tetragonal pyramids and TiO_6 octahedra.[11]

As a result of systematic synthesis studies following this approach, we have obtained new uranium silicates with open-framework structures. Here we report the synthesis and characterization of $Na_2(UO_2)(Si_4O_{10})\cdot 2.1H_2O$ (USH-1) and $RbNa(UO_2)(Si_2O_6)\cdot H_2O$ (USH-3).

Experimental

Synthesis

In a typical synthesis of USH-1, an aqueous solution of sodium silicate (1.04 ml, 14% NaOH, 27% SiO_2) was mixed with aqueous NaOH solution (0.82 ml, 4.24 M), $UO_2(NO_3)_2\cdot 6H_2O$ (523 mg) and H_2O (3 ml). The mixture was sealed in a Teflon-lined autoclave with an inner volume of 23 ml and was heated at 230 °C for 7 days. The product was recovered by washing with water and vacuum-filtering. USH-3 was similarly synthesized from a mixture of sodium silicate solution (0.64 ml, 14% NaOH, 27% SiO_2), aqueous RbOH solution (0.44 ml, 4.24 M), $UO_2(NO_3)_2\cdot 6H_2O$ (502 mg) and H_2O (3 ml). The mixture was heated at 230 °C for 10 days.

Characterization

The synthesis products were examined with a polarized optical microscope and a JEOL-JSM6400 scanning electron microscope. Chemical compositions were measured with a JEOL 8600 electron microprobe at 15 K eV, 10 μm beam diameter and 30 nA beam current, and by elemental analysis carried out by Galbraith Laboratories, Knoxville, TN. Thermogravimetric analysis (TGA) was carried out in a simulated air flow with a heating rate of 5 °C min^{-1}, on a TA Instruments Hi-Res 2950 system. Infrared spectra were collected with a Galaxy FTIR 5000 spectrometer using the KBr pellet method. UV–Vis–NIR diffuse reflectance spectra were measured with a Cary 500 spectrophotometer on powder samples at room temperature.

 DOI: 10.1039/b109878k

Table 1 Crystal data and structure refinement details

	USH-1	USH-3
Formula	$H_{4.2}$ $Na_2O_{14.1}Si_4U$	$H_2NaO_9RbSi_2U$
FW	626.20	548.69
Temperature/K	293(2)	293(2)
Wavelength/Å	0.71073	0.71073
Space group	*C*2/*m*	$P\bar{1}$
a/Å	12.7718(7)	7.3668(5)
b/Å	13.6139(7)	7.8691(6)
c/Å	8.2466(4)	8.1766(6)
α/°	90	78.024(1)
β/°	119.26(1)	75.013(1)
γ/°	90	83.741(1)
V/Å^3	1250.9(1)	447.14(6)
Z	4	2
Absorption coefficient	13.5 mm^{-1}	23.9 mm^{-1}
θ_{max}	28.23°	28.20°
Reflections collected	3906	2697
Independent reflections	1477	1932
R(int)	0.0438	0.0293
Data/parameters	1477/121	1932/131
Goodness-of-fit	1.064	1.143
$R1/wR2$ [$I > 2\sigma(I)$][a]	0.0456/0.1292	0.0469/0.1374
$R1/wR2$ (all data)[a]	0.0493/0.1339	0.0485/0.1391
Extinction coefficient	0.0021(4)	0.016(2)
Max. diff. peak /hole	2.88/−4.76 e Å^{-3}	4.14/−3.55 e Å^{-3}

[a] $R1 = \Sigma||F_o| - |F_c||/\Sigma|F_o|$, $wR2 = [\Sigma(w(F_o^2 - F_c^2)^2)/\Sigma(wF_o^2)^2]^{1/2}$.

Powder X-ray diffraction patterns were obtained using a Sintag XDS 2000 diffractometer and Cu-Kα radiation.

For crystal structure determination, single crystal X-ray diffraction data were measured on a SMART platform diffractometer equipped with a 1 K CCD area detector using graphite-monochromatized MoK_α radiation at 293 K. A hemisphere of data (1271 frames at 5 cm detector distance) was collected for each phase using a narrow-frame method with scan widths of 0.30° in ω and an exposure time of 30 s frame^{-1}. The first 50 frames were remeasured at the end of data collection to monitor instrument and crystal stability. The data were integrated using the Siemens SAINT program, with the intensities corrected for Lorentz factor, polarization, air absorption, and absorption due to variation in the path length through the detector faceplate.[12] Absorption corrections were made using the program SADABS.[13] The structures were solved and refined using SHELXTL.[14] For USH-1 some of the water molecules were found to be disordered. In the final refinements the total water content was fixed to 2.1 H_2O per formula unit observed from TGA data in order to refine relative occupancies of the disordered water oxygen sites. The occupancies of Na2 and Na3 of USH-1 were both refined to slightly higher than 50%, and were fixed at the maximum possible value 50% in the final refinements because of the too short atom distances (Na2–Na2: 2.98 Å, Na3–Na3: 2.05 Å). Thermal ellipsoids for Na2 and Na3 are much larger than Na1 because the former are disordered and the latter is ordered. Crystallographic and refinement details are summarized in Table 1.† Atom positions are given in Tables 2 and 4, and selected bond lengths in Tables 3 and 5.

Table 2 Atomic coordinates ($\times 10^4$) and equivalent isotropic displacement parameters (Å^2 $\times$ 10^3) for USH-1. *U*(eq) is defined as one third of the trace of the orthogonalized U_{ij} tensor

	x	*y*	*z*	*U*(eq)	Site-symm
Na(1)	0	1353(5)	0	29(1)	2
Na(2)	5000	−1093(17)	0	87(7)	2
Na(3)	−916(16)	5000	−5790(20)	54(4)	*m*
U	2500	2500	0	12(1)	−1
Si(1)	2288(1)	1121(1)	−3856(2)	10(1)	1
Si(2)	4456(2)	2195(2)	−3713(2)	10(1)	1
O(1)	2418(5)	1250(5)	−1856(8)	26(1)	1
O(2)	1904(6)	0	−4606(9)	15(1)	*m*
O(3)	0	3218(5)	5000	16(1)	2
O(4)	−1251(4)	1804(4)	−4567(7)	18(1)	1
O(5)	2717(5)	3363(4)	−1473(8)	20(1)	1
O(6)	3541(4)	1327(4)	−3831(7)	21(1)	1
O(7)	482(7)	2630(4)	−1611(11)	18(1)	1
Ow1	276(8)	0	8316(12)	33(2)	*m*
Ow2A	−1119(19)	5000	−6880(40)	44(5)	*m*
Ow2B	4060(20)	0	920(40)	49(8)	*m*
Ow2C	4590(60)	0	160(100)	40(20)	*m*

Table 3 Selected bond lengths [Å] for USH-1

U–O(5) ×2	1.806(5)	Na(1)–Ow1 ×2	2.434(7)
U–O(1) ×2	2.256(6)	Na(1)–O(7) ×2	2.443(8)
U–O(7) ×2	2.257(7)	Na(1)–O(5) ×2	2.581(5)
Si(1)–O(1)	1.584(6)	Na(2)–Ow2B ×2	2.26(2)
Si(1)–O(6)	1.614(5)	Na(2)–O(7) ×2	2.44(2)
Si(1)–O(4)	1.621(5)	Na(2)–O(6) ×2	2.793(6)
Si(1)–O(2)	1.630(3)	Na(2)–O(1) ×2	2.886(6)
Si(2)–O(4)	1.596(5)		
Si(2)–O(7)	1.599(8)		
Si(2)–O(3)	1.627(3)		
Si(2)–O(6)	1.632(5)		

Table 4 Atomic coordinates ($\times 10^4$) and equivalent isotropic displacement parameters (Å^2 $\times$ 10^3) for USH-3. *U*(eq) is defined as one third of the trace of the orthogonalized U_{ij} tensor

	x	*y*	*z*	*U*(eq)
Rb	1077(1)	4487(1)	2103(1)	24(1)
Na	3922(6)	8043(6)	7594(5)	23(1)
U(1)	5000	5000	5000	8(1)
U(2)	0	0	10000	10(1)
Si(1)	2148(3)	1384(3)	5628(3)	9(1)
Si(2)	−2104(3)	1402(3)	6491(3)	9(1)
O(1)	3127(9)	5420(9)	6840(8)	15(1)
O(2)	729(10)	−2273(9)	9778(9)	18(1)
O(3)	3533(9)	6928(8)	3217(8)	12(1)
O(4)	2236(9)	816(9)	7610(8)	13(1)
O(5)	3517(9)	2875(8)	4530(8)	13(1)
O(6)	−2(10)	2059(9)	5464(10)	16(1)
O(7)	−2789(9)	354(9)	5245(9)	17(1)
O(8)	1921(9)	−107(9)	11739(8)	14(1)
OW	4421(12)	2568(11)	309(10)	27(2)

Table 5 Selected bond lengths [Å] for USH-3

U(1)–O(1) ×2	1.819(6)	Rb–O(2)	2.877(7)
U(1)–O(5) ×2	2.240(6)	Rb–Ow	2.956(9)
U(1)–O(3) ×2	2.266(6)	Rb–O(6)	2.976(7)
		Rb–O(1)	2.989(6)
U(2)–O(2) ×2	1.843(7)	Rb–O(5)	3.014(6)
U(2)–O(4) ×2	2.234(6)	Rb–O(2)	3.137(7)
U(2)–O(8) ×2	2.236(6)	Rb–O(3)	3.183(6)
Si(1)–O(5)	1.597(7)	Na–Ow	2.297(9)
Si(1)–O(4)	1.606(6)	Na–O(5)	2.372(7)
Si(1)–O(7)	1.641(7)	Na–O(4)	2.391(8)
Si(1)–O(6)	1.644(7)	Na–O(1)	2.442(8)
		Na–O(2)	2.560(8)
Si(2)–O(3)	1.609(6)	Na–O(7)	2.689(8)
Si(2)–O(8)	1.615(6)		
Si(2)–O(7)	1.636(7)		
Si(2)–O(6)	1.641(7)		

†CCDC reference numbers 176119–176120. See http://www.rsc.org/suppdata/jm/b1/b109878k/ for crystallographic files in .cif or other electronic format.

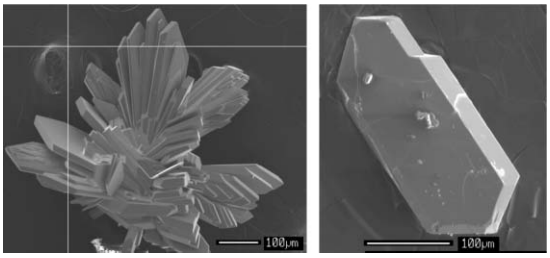

Fig. 1 SEM images of typical crystals of USH-1(left) and USH-3 (right).

Results and discussion

Synthesis

Pale yellow plate-like crystals of USH-1 with maximum dimensions of 0.4 mm were obtained. The product was confirmed to be pure by comparing the measured powder X-ray pattern with the one simulated from the refined crystal structure data. The yield is over 90% based on uranium in an optimum experiment. We noticed that the yield of USH-1 is sensitive to the NaOH content of the starting mixture. Increasing the U : Si ratio of the reagents led to formation of uranium-rich phases such as Na-boltwoodite ($NaUO_2$-$SiO_3OH{\cdot}xH_2O$).[15] Pale yellow polyhedral crystals of USH-3 were obtained as a minor phase together with USH-1 and USH-2. The latter is another novel uranium silicate that will be reported elsewhere. Efforts to synthesize phase pure USH-3 and to increase the yield by adjusting starting mixture compositions have not yet been successful. Fig. 1 shows SEM images of typical crystals of USH-1 and USH-3.

Characterization

The measured chemical compositions are consistent with the title formula derived from crystal structure refinements for both compounds. TGA data measured from 30–500 °C for USH-1 show that between 30 and 200 °C the sample gradually loses about 1.5% weight, corresponding to approximately 0.5 H_2O per formula unit. Starting from ~200 °C the dehydration becomes much faster and ends at ~270 °C. The total weight loss of 6.1% corresponds to 2.1 H_2O per formula unit, and is consistent with the results of single crystal structure refinements. In the final structure refinements the total water content was fixed to the TGA result in order to refine relative occupancies of the disordered water positions. The powder X-ray diffraction pattern measured for the sample after TGA (with further heating at 500 °C for 2 h) is closely similar to that measured for the original sample, showing the good thermal stability of the structure.

Fig. 2 shows the infrared spectra of USH-1 and USH-3. The bands observed between 700–900 cm^{-1} are most probably due to stretching vibrations of the $(UO_2)^{2+}$ ions.[16,17] The strong bands between 900–1200 cm^{-1} and the bands between 700–400 cm^{-1} are mainly due to the stretching and bending vibrations of the silicate groups, respectively. The bands in the regions 1600–1700 cm^{-1} and 3000–3600 cm^{-1} are typical for water molecules. The water bands observed for USH-1 are broader than USH-3 because the water molecules in the former are disordered. The weak band at 1385 cm^{-1} may be due to the presence of SiOH groups at defect sites and particle surfaces.[17]

The UV–Vis–NIR spectrum for USH-1 is shown in Fig. 3. The absorption bands in the region 200–500 nm are characteristic for U^{6+}. No band in the visible region typical for low valent uranium (>500 nm) is detected.[18,19] Absorption bands of water are observed in the region 1100–2000 nm. Similar bands were previously assigned to self-hydrogen bonded water in clay minerals.[20]

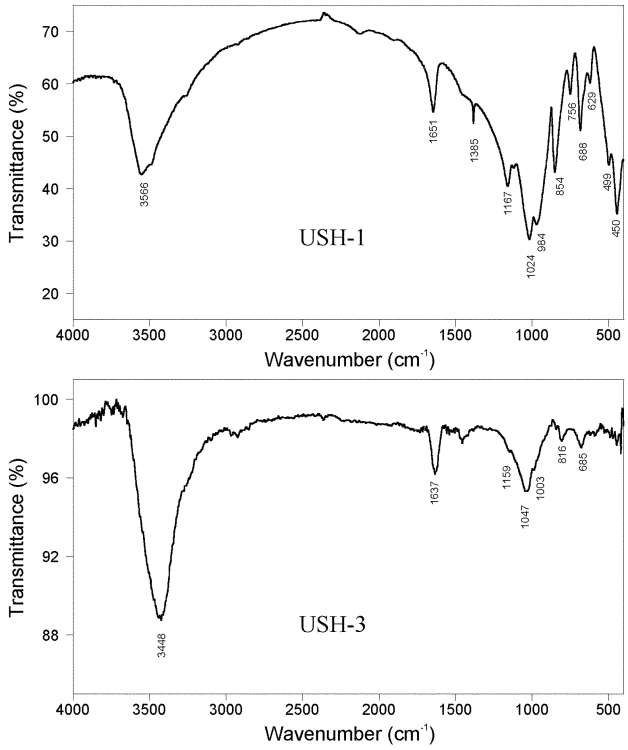

Fig. 2 The infrared spectra of USH-1 and USH-3.

Crystal structures

In the structure of USH-1, single layers of SiO_4 tetrahedra are cross-linked by individual UO_6 tetragonal bipyramids to form a framework. The sodium ions and water molecules are located within the voids of the framework (Fig. 4). Fig. 5 shows the coordination environments of the framework cations. The two independent SiO_4 tetrahedra have Si–O bond lengths 1.584–1.632 Å and O–Si–O angles 104.8–113.7°. The UO_6 tetragonal bipyramid is centrosymmetric and has two apical uranyl bonds of 1.806 Å and four equatorial U–O bonds of 2.256–2.257 Å. The primary unit of the silicate single layer is a centrosymmetric 4-ring formed by four SiO_4 tetrahedra, each sharing two corners with two others. The 4-ring is connected to four neighboring 4-rings by sharing the remaining corners of the tetrahedra to form the single layer that has 8-ring voids (Figs. 4, 8). The interlayer UO_6 tetragonal bipyramids cross-link neighboring silicate layers to form the framework by sharing their equatorial oxygen corners with the SiO_4 tetrahedra. The stacking of the silicate layers is by simple translation along [001]. As a result, the 8-ring voids are lined up to form two different 1-dimensional channels along [001] with apertures of about 2.1 × 5.0 Å and 1.8 × 4.4 Å, respectively. The extra-framework ions and water molecules located in the narrower channels (Na1 and Ow1) are ordered while those located in the wider channels are disordered.

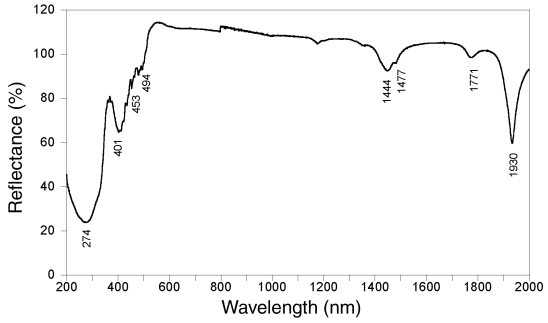

Fig. 3 UV–Vis–NIR diffuse reflectance spectra of USH-1.

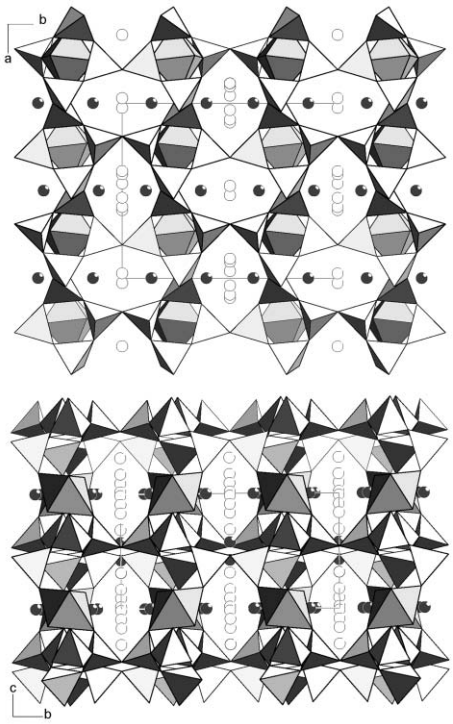

Fig. 4 Two projections of the structure of USH-1. Open and filled circles represent water oxygen and sodium atom positions, respectively.

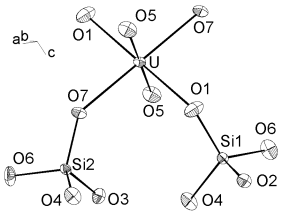

Fig. 5 Coordination environments of Si and U in USH-1 Thermal ellipsoids are plotted at 50% probability.

USH-1 is closely related to $KNa_3(UO_2)_2(Si_4O_{10})_2(H_2O)_4$ recently reported by Burns *et al.*,[21] which was discovered from vapor hydration of a U-doped borosilicate waste glass. The framework structures of the two phases are basically the same, but the latter has a non-centrosymmetric space group symmetry probably caused by substitution of K for Na. Independently, Burns has also synthesized the phase containing only Na.[22]

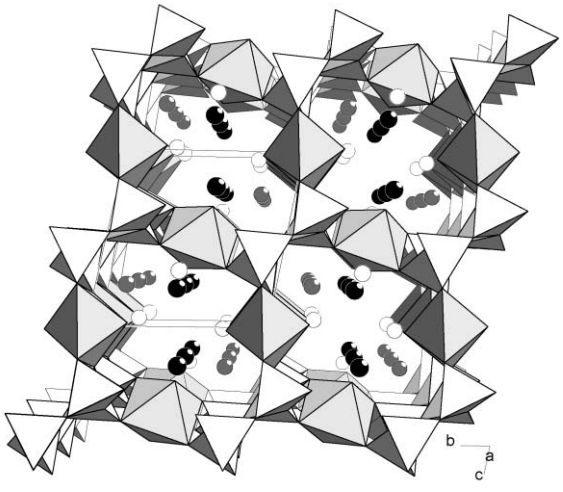

Fig. 6 A view of the structure of USH-3. Open circles represent water oxygen. Black- and grey-filled circles represent Rb and Na atoms respectively.

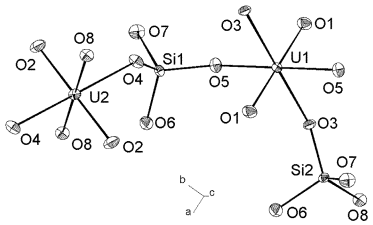

Fig. 7 Coordination environments of Si and U in USH-3. Thermal ellipsoids are plotted at 50% probability.

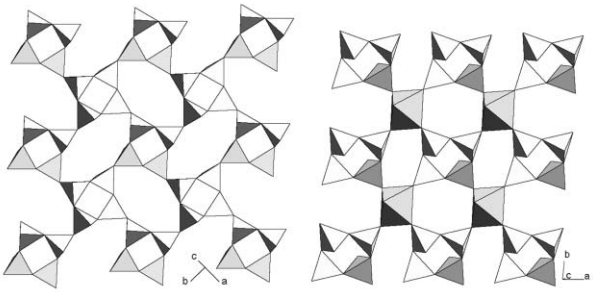

Fig. 8 Comparison of the silicate layer of USH-1 (left) and the (001) hybrid layer of USH-3 (right). The latter can be derived by replacing a half 4-rings of the former with uranium oxygen tetragonal bipyramids.

The structure of USH-3 consists of individual tetrahedral 4-rings interconnected by UO_6 tetragonal bipyramids (Fig. 6). Fig. 7 shows the coordination environments of the framework cations. The SiO_4 tetrahedra have Si–O bond lengths 1.597–1.644 Å and O–Si–O angles 107.0–114.6°. Both UO_6 tetragonal bipyramids are centrosymmetric and have apical uranyl bonds of 1.819–1.843 Å and equatorial U–O bonds of 2.234–2.266 Å. If one half of the 4-rings in the USH-1 silicate layer are each replaced by a UO_6 tetragonal bipyramids, a hybrid layer will be obtained which is the basis of the USH-3 structure (Fig. 8). The framework of USH-3 is formed by stacking these hybrid layers along [001] and cross-linking them with additional UO_6 tetragonal bipyramids. While the UO_6 bipyramid within the hybrid layer is linked to four tetrahedral 4-rings, the interlayer UO_6 bipyramid is connected to two tetrahedral 4-rings from two adjacent layers. SiO_4 tetrahedra and UO_6 tetragonal bipyramids outline 1-dimensional channels along [100] which have an aperture of about 1.7 × 2.9 Å. Extra-framework Na and Rb ions and water molecules are located in the channels and are all ordered. Relatively strong hydrogen bonding may occur between water molecules and framework oxygen atoms (Ow–O8: 2.81 Å, Ow–O3: 2.86 Å).

The silicate layers of USH-1 and cavansite are similar, both consisting of 4-rings and 8-rings, but they have different orientations of tetrahedra. In USH-1 the two tetrahedra connected to the interlayer UO_6 bipyramid are from two 4-rings and are separated by a third tetrahedron. In contrast, the two tetrahedra connected to the interlayer VO_5 pyramid in cavansite are from the same edge of a 4-ring. This difference may be due to the ion size of U^{6+} which is larger than V^{4+}. In USH-3 the silicate 4-rings of the (001) hybrid layer are separated from each other, and the interlayer connection is similar to cavansite, *i.e.*, the two tetrahedra connected to the interlayer UO_6 bipyramids are from the same edge of a 4-ring. The equatorial U–O bonds of the interlayer UO_6 bipyramids in USH-3 are considerably shorter than in USH-1.

Conclusions

Two new open-framework uranium silicates have been obtained by hydrothermal synthesis at mild temperatures. Their crystal structures are based on a similar building principle to those observed in the vanadium silicates VSH-1 and VSH-2. The hexavalent uranium ions have tetragonal bipyramidal coordination with linear O=U=O group in these compounds. The equatorial oxygen atoms of the UO_6 bipyramids have similar bonding capability to those of the VO_5 tetragonal pyramids. Our preliminary results suggest that these phases may represent first examples of a large family of new uranium silicates based on well-defined structural principles.

Acknowledgement

We thank the National Science Foundation (DMR9805881), the R.A. Welch Foundation for financial support. This work made use of MRSEC/TCSUH Shared Experimental Facilities supported by the National Science Foundation under Award Number DMR-9632667 and the Texas Center for Superconductivity at the University of Houston.

References

1 H. V. Bekkum, E. M. Flanigen and J. C. Jansen, *Introduction to Zeolite Science and Practice*, Elsevier, Amsterdam, 1991.
2 S. T. Wilson, B. M. Lok, C. A. Messina, T. R. Cannan and E. M. Flanigen, *J. Am. Chem. Soc.*, 1982, **104**, 1146; C. Baerlocher, W. M. Meier and D. H. Olsen, *Atlas of Zeolite Framework Types*, Elsevier, Amsterdam, 2001.
3 R. C. Haushalter, K. G. Strohmaier and F. W. Lai, *Science*, 1989, **246**, 1289; A. K. Cheetham, G. Férey and T. Loiseau, *Angew. Chem., Int. Ed.*, 1999, **38**, 3268.
4 R. J. Francis, M. J. Drewitt, P. S. Halasyamani, C. Ranganathachar, D. O'Hare, W. Clegg and S. J. Teat, *Chem. Commun.*, 1998, 279.
5 J. Rocha and M. W. Anderson, *Eur. J. Inorg. Chem.*, 2000, 801.
6 S. M. Kuznicki, V. A. Bell, S. Nair, H. W. Hillhouse, R. M. Jacubinas, C. M. Braunbarth, B. H. Toby and M. Tsapatsis, *Nature*, 2001, **412**, 720.
7 X. Wang, L. Liu and A. J. Jacobson, *Angew. Chem., Int. Ed.*, 2001, **40**, 2174.
8 H. T. Evans, *Amer. Mineralog.*, 1973, **58**, 412.
9 R. J. Francis and A. J. Jacobson, *Chem. Mater.*, 2001, **13**, 4676.
10 H. Li, M. Eddaoudi, J. Plévert, M. O'Keeffe and O. M. Yaghi, *J. Am. Chem. Soc.*, 2000, **122**, 12409.
11 R. Philippou and M. W. Anderson, *Zeolite*, 1996, **16**, 98; G. Cruciani, P. De Luca, A. Nastro and P. Pattison, *Microporous Mesoporous Mater.*, 1998, **21**, 143; C. Braunbarth, H. W. Hillhouse, S. Nair, M. Tsapatsis, A. Burton, R. F. Lobo, R. Jacubinas and S. M. Kuznicki, *Chem. Mater.*, 2000, **12**, 1857.
12 SAINT, Program for Data Extraction and Reduction, Siemens Analytical X-ray Instruments Inc., Madison, USA, 1996.
13 G. M. Sheldrick, SADABS, Program for Siemens Area Detector Absorption Corrections, University of Gottingen, Germany, 1997.
14 G. M. Sheldrick, SHELXTL, Program for Refinement of Crystal Structures, Siemens Analytical X-ray Instruments Inc., Madison, USA, 1994.
15 R. Vochten, N. Blaton, O. Peters, K. V. Springel and L. V. Haverbeke, *Can. Mineral.*, 1997, **35**, 735.
16 E. P. Plesko, B. E. Scheetz and W. B. White, *Am. Mineral.*, 1992, **77**, 431.
17 J. Čfejka, *Rev. Mineral.*, 1999, **38**, 522.
18 W. T. Carnall, *Gmelin Handbuch der Anorganischen Chemie*, 1982, **vol. A5**, p. 69.
19 J. M. Hanchar, *Rev. Mineral.*, 1999, **38**, 499.
20 L. M. Coyne, J. L. Bishop, T. Scattergood, A. Bannin, G. Carle and J. Orenberg, *ACS Symp. Ser.*, 1990, **415**, 407.
21 P. C. Burns, R. A. Olson, R. J. Finch, J. M. Hanchar and Y. Thibault, *J. Nucl. Mater.*, 2000, **278**, 290.
22 P. C. Burns, personal communication.